Electronic Supplementary Information

The 2D PN Junction Driven Out-of-Equilibrium

Ferney A. Chaves, Pedro C. Feijoo and David Jiménez

Departament d'Enginyeria Electrònica, Escola d'Enginyeria,
Universitat Autònoma de Barcelona, Campus UAB, 08193 Bellaterra, Spain.

S1. Details of the numerical model used for the electrical simulation of 2D diodes

Fig. 1 of the main text represents the physical structure of the 2DJ considered in this work. The semiconductor lays in the plane $z = 0$, where there is an abrupt junction of p-type and n-type semiconductors at $x = 0$. The device width W along the y-axis is large enough to consider the independence of its properties on that direction. The metal electrodes at the edges of the device $(x_{min}, y, 0)$ and $(x_{max}, y, 0)$ are considered to make perfect ohmic contacts and supply a ground reference potential to the right edge and a potential V to the left edge (see Fig. S1). The non-linear Poisson's equation:

$$-\nabla^2\phi(x,z;V) = \sigma(\phi;V)\delta(z)/\epsilon_{eff}, \tag{S1}$$

describes the 2DJ electrostatics, where $\phi(x,z;V)$ is the 2D electrostatic potential distribution in the xz-plane when a bias V is applied to the device, σ is the space charge density, ϵ_{eff} is the effective dielectric permittivity of the insulating media surrounding the junction and $\delta(z)$ is the Dirac delta function. The effective permittivity ϵ_{eff} is calculated as the mean value between the permittivity of the dielectric above the junction and the permittivity of the dielectric below the junction. The sheet charge density is σ, where q, n and p are the elementary charge, and the electron and hole surface densities, respectively. By assuming complete ionization, N_D and N_A are the surface doping densities of donors and acceptors, respectively. Here, we have assumed chemically doped 2D semiconductors. Now, by integrating Eq. S1 along z and using the Dirac delta function properties, the electrostatic problem can be transformed into the following Laplace's equation:

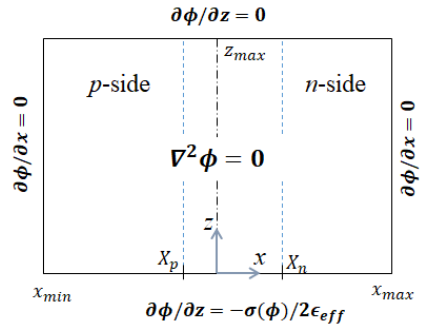

Fig. S1 Calculation window of the 2D Poisson's equation and considered boundary conditions

$$\nabla^2\phi(x,z;V)=0, \tag{S2}$$

along with the boundary conditions: $\partial\phi/\partial z=-\sigma(\phi)/2\epsilon_{eff}$ at $z=0$, and Neumann-like boundary conditions for the rest of the domain boundaries, as shown in Fig. S1, which illustrates the window of the numerical calculation. Additional details about the method to solve the Laplace's equation can be found in our previous work.[1]

For the description of the 2DJ electrodynamics along the lateral dimension x, the drift and diffusion currents contributions must be considered for both electron and hole currents. Thus, the 1D electron and hole current densities are determined by the following equations:

$$J_n=-q\mu_n n\left[\frac{d\varphi}{dx}-\frac{D_n}{\mu_n n}\frac{dn}{dx}\right]=-q\mu_n n\frac{dV_n}{dx}, \tag{S3a}$$

$$J_p=-q\mu_p p\left[\frac{d\varphi}{dx}+\frac{D_p}{\mu_p p}\frac{dp}{dx}\right]=-q\mu_p p\frac{dV_p}{dx}, \tag{S3b}$$

where $\mu_{n(p)}$ and $D_{n(p)}$ are the electron (hole) mobility and diffusion coefficient, respectively, $\varphi(x)=\phi(x,0;V)$ is the in-plane electrostatic potential under the quasi-steady-state approximation and $V_{n(p)}(x)$ is the electron (hole) quasi-Fermi potentials profile. φ and $V_{n(p)}$ are related to the local intrinsic energy E_i and electron (hole) Fermi energy as $E_i(x)=-q\varphi$ and $E_{Fn(p)}(x)=-qV_{n(p)}$, respectively. The boundary conditions set V_n and V_p to zero at the right edge of the n-side ($x=x_{max}$) and V at the left edge of the p-side ($x=x_{min}$). The local electron and hole densities can be written in terms of the electrostatic and the quasi-Fermi potentials as follow:

$$n(x)=n_s log\left\{1+e^{(q\varphi(x)-qV_n(x)-E_g/2)/kT}\right\} \tag{S4a}$$

$$p(x)=n_s log\left\{1+e^{(-q\varphi(x)+qV_p(x)-E_g/2)/kT}\right\}, \tag{S4b}$$

where $n_s=g_{2D}kT$, with g_{2D} the band–edge density of states (DOS), k the Boltzmann constant and T the absolute temperature.[1] As an example, g_{2D} for single layer MoS_2 is about 5×10^6 eV^{-1}μm^{-2}.[2] All the simulations in this work have been done assuming room temperature ($T=300$ K).

Finally, in order to complete our model, we need to consider the conservation of the mobile charge through the continuity equations:

$$\frac{dJ_n}{dx}=qU(n,p) \tag{S5a}$$

$$\frac{dJ_p}{dx}=-qU(n,p), \tag{S5b}$$

where U is the net recombination rate mediated by capture and emission of carriers at trap centers located in the band gap of the semiconductor. Note that, from Eqs. S5, then $J(x)=J_n(x_0)+J_p(x_0)=J=const$. Based on the Shockley-Read-Hall model, like in 3D semiconductors,[3] the following expression for U can be obtained (for the non-degenerated case):

$$U=\frac{pn-n_i^2}{\tau_p(n+n_i)+\tau_n(p+n_i)} \tag{S6}$$

where $\tau_{n(p)}$ represents the minority electron (hole) lifetime, at low-level injection, and $n_i=n_s log\left[1+exp\left(-E_g/2kT\right)\right]$ is the 2D intrinsic electron density.

Our method solves Eqs. S2-S5 in a self-consistent way in order to get $\phi(x,z), V_n(x), V_p(x), J_n(x), J_p(x)$ for a given applied bias V. Details about the algorithm used to solve the abovementioned set of equations, are given in the following diagram:

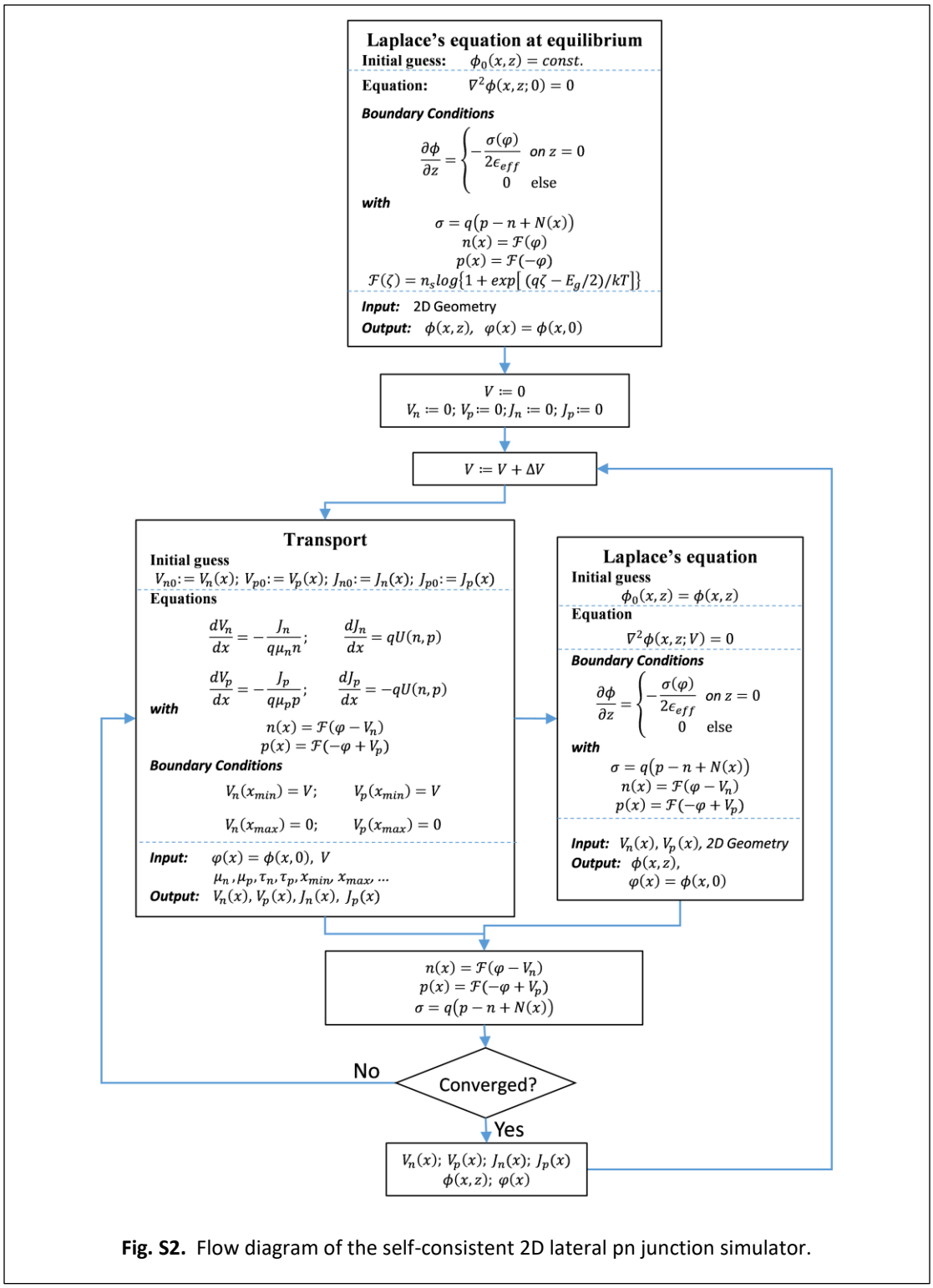

Fig. S2. Flow diagram of the self-consistent 2D lateral pn junction simulator.

For both reverse bias and forward bias the algorithm starts from the solution of the 2D Poisson's equation at thermal equilibrium in the x-z plane by using an elementary initial guess $\phi_0(x,z) = const.$

To find the solution $[\varphi_k(x), V_{n,k}(x), V_{p,k}(x), J_{n,k}(x), J_{p,k}(x)]$ to the system of equations at the applied bias V_k, where $x \in [x_{min}, x_{max}]$, l iterations are needed before the algorithm converges. In the iteration i ($i = 1,2\ 3,..,l$), firstly, the 1D transport's equations (Drift-Diffusion + Continuity) are solved under the boundary conditions imposed by the quasi-Fermi potentials, to find $[V^i_{n,k}(x), V^i_{p,k}(x), J^i_{n,k}(x), J^i_{n,k}(x)]$. In this point, the initial guess is the solution of the previous iteration $[V^{i-1}_{n,k}(x), V^{i-1}_{p,k}(x),\ J^{i-1}_{n,k}(x),\ J^{i-1}_{n,k}(x)]$ and the used electrostatic potential is that from the previous iteration $\varphi^{i-1}_k(x)$. Secondly, the 2D out-of-equilibrium Laplace's equation is solved in the x-z plane, under the boundary conditions given in Fig. S1, to find $\phi_k(x,z)$. At this point, the initial guess is the electrostatic potential $\phi^{i-1}_k(x,z)$ found in the previous iteration and the quasi-Fermi potentials are those from the present iteration $V^i_{n,k}(x), V^i_{p,k}(x)$. Then, the charge density distribution $\sigma^i_k(x)$ is calculated with the new solution $[\varphi_k(x), V_{n,k}(x), V_{p,k}(x)]$ and compared with the charge density distribution $\sigma^{i-1}_k(x)$ of the previous iteration by means of the relative error defined as:

$$\varepsilon^i_k = \left\{ \frac{\int_{x_{min}}^{x_{max}} \left[\sigma^i_k(x) - \sigma^{i-1}_k(x)\right]^2 dx}{\int_{x_{min}}^{x_{max}} \left[\sigma^{i-1}_k(x)\right]^2 dx} \right\}^{1/2} \tag{S7}$$

When the algorithm converges for the bias V_k, the solution of the system $[\varphi_k(x), V_{n,k}(x), V_{p,k}(x), J_{n,k}(x), J_{p,k}(x)]$ serves as the initial guess for the first iteration of the self-consistency at bias V_{k+1}. This way, the algorithm is able to find the 2D electrostatic potential $\phi(x,z)$, the 1D electrostatic potential $\varphi(x) = \phi(x,0)$, the quasi-Fermi potentials $V_n(x)$ and $V_p(x)$, the density currents $J_n(x)$ and $J_p(x)$, and the total current $J = J_n(x_o) + J_p(x_o)$, for any given bias point . Here, x_o is any point belonging to the interval $[x_{min}, x_{max}]$.

S2. Discussion on the effective depletion layer width.

In this section we have compared Nipane's analytical model for the electrostatic potential and sheet charge density with our numerical model results.[4] We have carried out simulations of 2DJs for different levels of doping, resulting in diodes with different degree of asymmetry.

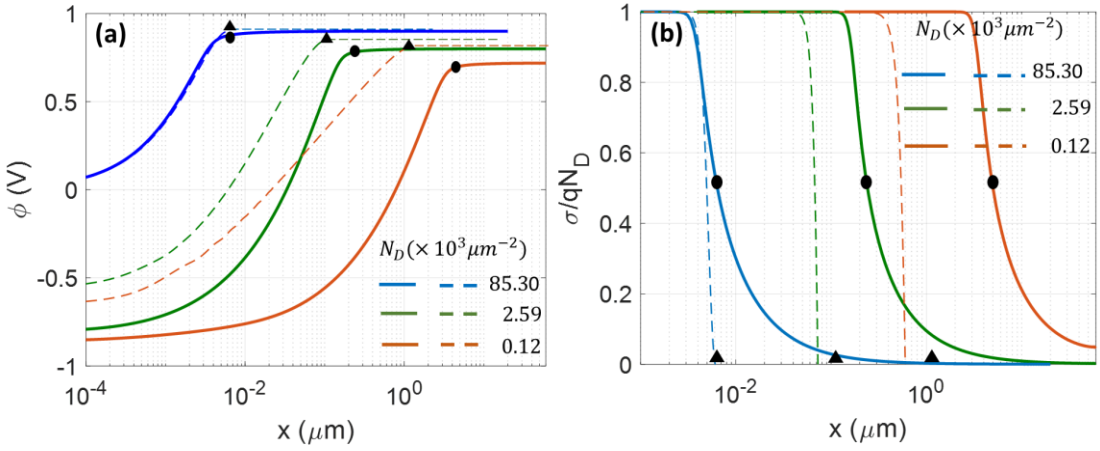

Fig. S3 Comparison between Nipane's analytical model and numerical results in this work (a) Electrostatic potential profile. (b) Normalized sheet charge density. Solid lines: numerical model. Dashed lines: Nipane's analytical model. Only the n-side of the 2DJ is shown. Circles indicate the EDL width given by $W_{D,eff(2)}$ determined under the numerical condition $\sigma/qN_D \sim 0.56$ and triangles indicate the EDL width given by $W_{D,eff(1)}$ from Nipane's analytical model (see Eq. 2 of the main text).

Fig. S3 shows both the electrostatic potential and the normalized sheet charge density as a function of the position for the considered 2DJ in equilibrium. We have fixed $N_A = 85.3 \times 10^3\ \mu m^{-2}$ in the p-side and assumed three different doping level in the n-side, namely $N_D = 85.3 \times 10^3, 2.59 \times 10^3$ and $0.12 \times 10^3\ \mu m^{-2}$, which correspond to equilibrium potentials $\varphi_p = -0.9\,V$ and $\varphi_n = 0.9, 0.8$ and $0.72\,V$, respectively. The rest of the parameters used in the simulations are those of the device 2DJ2 in Table I of the main manuscript. Solid lines correspond to numerical simulations with the model presented in this work and dashed lines to Nipane's analytical model.[4] Fig. S3 shows that Nipane's analytical model fits very well to the simulations in the symmetric case, although accuracy is progressively loss as the diode becomes more asymmetric, even resulting in unphysical negative sheet charge densities.

From the results shown in Fig. S3, the n-side depletion widths can be determined from $W_{D,eff(1)}$ and $W_{D,eff(2)}$, respectively. They have been marked as triangles and circles, respectively. The value of the calculated n-type depletion widths are given in the following table, where an increasing discrepancy can be noted as the diode becomes more asymmetric:

Table S1. Effective depletion layer width vs doping concentration.

$N_D\ (\times 10^3 \mu m^{-2})$	$W_{D,eff(1)}(\mu m)$	$W_{D,eff(2)}(\mu m)$
85.3	0.006	0.006
2.59	0.1	0.2
0.12	1.3	4.6

S3. Edge effects in 2DJs

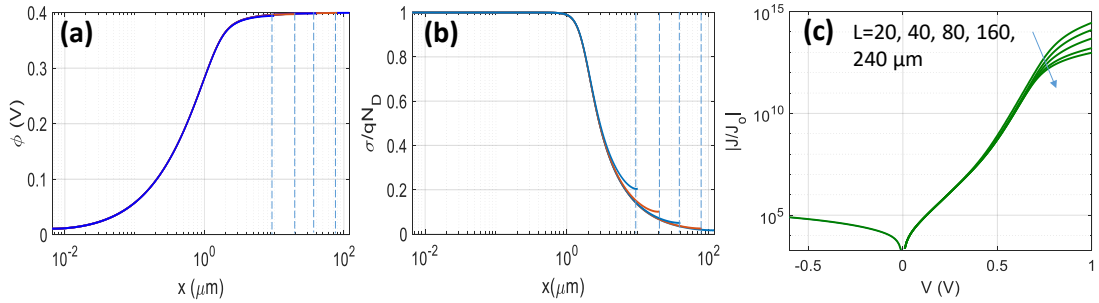

Fig. S4 Edge effects in 2DJs: simulated (a) electrostatic potential and (b) relative sheet charge density along the n-side together with the (c) J-V characteristics corresponding to the 2DJ1 device (described in Table I of the main manuscript) assuming different lengths covering both short and long diodes cases.

Given the larger transition region L_{2D} exhibited by 2DJs compared with that of the 3DJs, as shown in Fig. 3 of the main text, it is interesting to discuss the possible impact of considering a 2D diode whose length is shorter than the diffusion length, i.e. we are interested in unveiling the impact of edge effects on its performance. For this purpose, we have carried out simulations for the device 2DJ1 (Table I of main text) with lengths ranging from 20 to 240 µm, for which the electron and hole diffusion lengths are L_n~27 µm and L_n~13.5 µm, respectively. Thus, we have a "short diode" for the 20 µm case, relative to L_n and L_p, a "semi-short diode" for the 40 µm case and a "long diode" for the rest of considered cases. It is worth noticing that in every case the EDL width is smaller than the device length. Figs. S4a and S4b show the electrostatic potential and sheet charge density profiles at equilibrium for the 2DJ1 device. Fig. S4c shows the corresponding J-V curves, revealing that at bias dominated by G-R processes (reverse and forward bias up to approx. 0.4V) there is not

impact of edge effects, and at bias dominated by diffusion current ($V > 0.4$V) the impact is minimal. As expected, the edge effects are significant in the region dominated by series resistance, where the longer the device the smaller the current.

S4. Impact of the interface states

In this Section we discuss the impact of interface states between the 2D semiconductor and the surrounding dielectric. To take into account those interface states, we have added an additional interface trapped charge σ_{int} to the total charge already considered in the Poisson's equation:

$$\sigma = q(p - n + N_D - N_A) + \sigma_{int} \tag{S8}$$

We have assumed an interface density of acceptor and donor defects given by $D_{it,A}(E - E_i)$ and $D_{it,D}(E - E_i)$, respectively. At equilibrium, single Fermi level E_F for both acceptor and donor defects can be considered. If the acceptor state is occupied by an electron, it contributes with a negative charge to the interface charge, so the total acceptor defects' contribution to the interface charge can be calculated as:

$$\sigma_{int,A}(E_F, E_i) = -q\int_{-\infty}^{\infty} D_{it,A}\,(E - E_i) f_{FD}(E - E_F, T)dE = -q\int_{-\infty}^{\infty} D_{it,A}\,(\epsilon) f_{FD}(\epsilon + E_i - E_F, T)d\epsilon$$
$$= \sigma_{int,A}(E_F - E_i) \tag{S9}$$

Analogously, if the donor state are unoccupied, it contributes with a positive charge, so the donor defects' contribution to the interface charge can be written as:

$$\sigma_{int,D}(E_F, E_i) = +q\int_{-\infty}^{\infty} D_{it,D}\,(E - E_i)[1 - f_{FD}(E - E_F, T)]dE$$
$$= +q\int_{-\infty}^{\infty} D_{it,D}\,(\epsilon)[1 - f_{FD}(\epsilon + E_i - E_F, T)]d\epsilon$$
$$= \sigma_{int,D}(E_F - E_i), \tag{S10}$$

where $f_{FD}(E, T)$ is the occupation probability. Expression (S8) and (S9) can be conveniently simplified after applying the following assumptions:

Assumption 1 (simplification of the Fermi-Dirac distribution):

$$f_{FD}(E - E_F, T) \approx 1 \text{ for } E < E_F$$
$$f_{FD}(E - E_F, T) \approx 0 \text{ for } E > E_F \tag{S11}$$

$$\sigma_{int,A}(E_F - E_i) = -q\int_{-\infty}^{\infty} D_{it,A}\,(E - E_i) f_{FD}(E - E_F, T)dE = -q\int_{-\infty}^{E_F} D_{it,A}\,(E - E_i)dE$$

$$\sigma_{int,D}(E_F - E_i) = +q\int_{-\infty}^{\infty} D_{it,D}\,(E - E_i)[1 - f_{FD}(E - E_F, T)]dE = +q\int_{E_F}^{\infty} D_{it,D}\,(E - E_i)dE \tag{S12}$$

Assumption 2 (the density of defects is constant in the bandgap)

$$D_{it,A}(E - E_i) = D_{it,A} \text{ for } -E_g/2 < E - E_i < E_g/2$$
$$D_{it,D}(E - E_i) = D_{it,D} \text{ for } -E_g/2 < E - E_i < E_g/2 \tag{S13}$$

$$\sigma_{int,A}(E_F - E_i) = -q\int_{-\infty}^{E_F} D_{it,A}\,(E - E_i)dE = -q\int_{E_i - E_g/2}^{E_F} D_{it,A}\,dE = -qD_{it,A}\left(E_F - E_i + E_g/2\right)$$

$$\sigma_{int,D}(E_F - E_i) = +q\int_{E_F}^{\infty} D_{it,D}\,(E - E_i)dE = +q\int_{E_F}^{E_i + E_g/2} D_{it,D}\,dE = +qD_{it,D}\left(E_i + E_g/2 - E_F\right) \quad \text{(S14)}$$

So, the total charge at the interface can be written as:

$$\sigma_{int} = \sigma_{int,A}(E_F - E_i) + \sigma_{int,D}(E_F - E_i) \approx -qD_{it,A}\left(E_F - E_i + E_g/2\right) + qD_{it,D}\left(E_i + E_g/2 - E_F\right)$$

$$\sigma_{int} = -q\left(D_{it,A} + D_{it,D}\right)(E_F - E_i) + q\left(D_{it,D} - D_{it,A}\right)E_g/2$$

$$\sigma_{int} = -qD_{it}(E_F - E_i) + \sigma_{int,0} \quad \text{(S15)}$$

So far, we have assumed that the 2DJ is at equilibrium, but what happens if the device is driven out-of-equilibrium? In such a case the Fermi level (E_F) splits into different quasi-Fermi levels for electrons (E_{Fn}) and holes (E_{Fp}), respectively. In equilibrium the interface trapped charge can be expressed as

$$\sigma_{int} = -qD_{it}(-qV + q\varphi) + \sigma_{int,0} = -q^2 D_{it}(\varphi - V) + \sigma_{int,0}, \quad \text{(S16)}$$

so we propose to use the average between both quasi-Fermi levels for the out-of-equilibrium case:

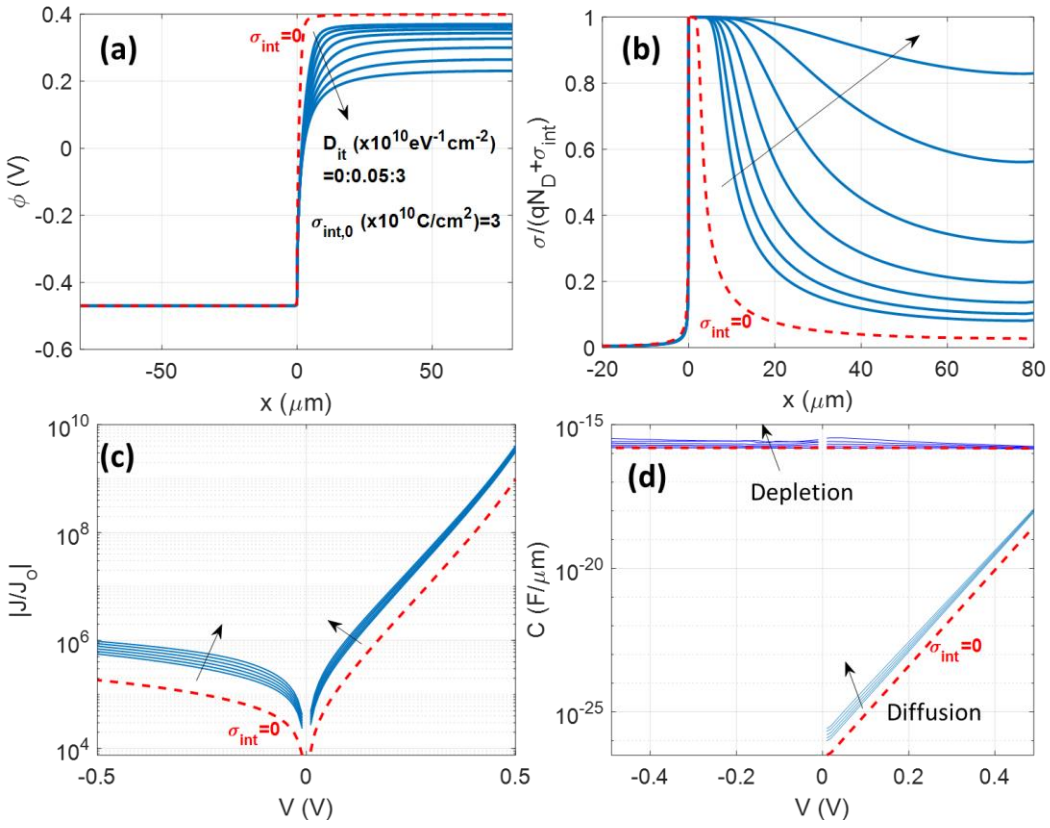

Fig. S5 Effect of the interface states in 2DJ: simulated (a) electrostatic potential, (b) sheet charge density, (c) J-V characteristics and (d) capacitances, corresponding to the 2DJ2 device described in Table I of the main manuscript. Dashed red lines correspond to the case without interface states for reference.

$$\sigma_{int}(\varphi, V_n, V_p) = -q^2 D_{it}\left(\varphi - \frac{V_n+V_p}{2}\right) + \sigma_{int,0}, \quad \text{(S17)}$$

where D_{it} is the density of interface states (eV^{-1} cm^{-2}) and $\sigma_{int,0}$ is the constant sheet density in the interface (C cm^{-2}).

Fig. S5 shows the result of our simulations taking into account interface states effects on the different electrical magnitudes for the exemplary device 2DJ2 described in the Table I of the manuscript. Dashed red lines correspond to the case without any interface trapped charge $\sigma_{int} = 0$ for comparison purposes. As discussed in the main text (Fig. 11), there is an increasing of the effective depletion layer with the density of interface defects located between the surrounding dielectric and the 2D semiconductor. Remarkably, this effect is not present in 3DJs.

Fig. S6 shows the interface charge effect on the dependency of the diode forward and reverse currents with the surrounding dielectric medium. In this case the simulations have been done for the symmetric device 2DJ3 described in Table I of the manuscript. The curves corresponding to densities of interface states different to zero (dashed lines), are compared with the case D_{it}=0 (solid lines) described in the inset of Fig. 12 of the manuscript. This result exhibits an expected slight detriment of the ratio I_{on}/I_{off} with the interface charge.

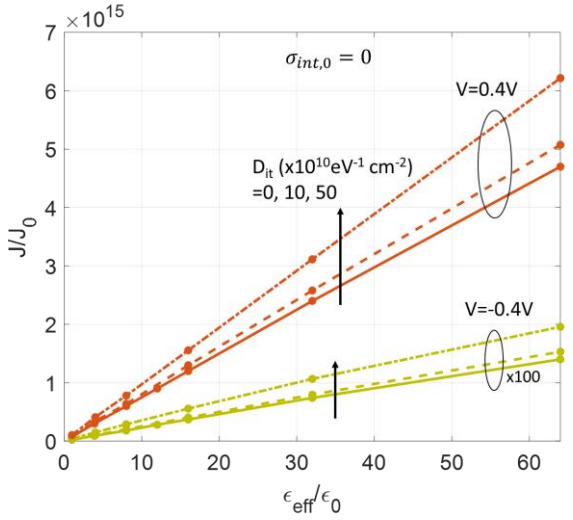

Fig. S6 Forward and reverse currents vs dielectric constant of the surrounding medium for different values of interface charge density D_{it}. $\sigma_{int,0} = 0$ has been assumed in all the cases.

REFERENCES

1 F. A. Chaves and D. Jiménez, Electrostatics of two-dimensional lateral junctions, *Nanotechnology*, 2018, **29**, 275203.

2 N. Ma and D. Jena, Carrier statistics and quantum capacitance effects on mobility extraction in two-dimensional crystal semiconductor field-effect transistors, *2D Mater.*, 2015, **2**, 015003.

3 Y. Taur and T. H. Ning, *Fundamentals of Modern VLSI Devices, 2nd Edition, Cambridge University Press*, 2013.

4 A. Nipane, S. Jayanti, A. Borah and J. T. Teherani, Electrostatics of lateral p-n junctions in atomically thin materials, *J. Appl. Phys.*, 2017, **122**, 194501.